Supporting Information

Anisotropically Enhanced Second Harmonic Generation in a WS_2 Nanoparticle Driven by Optical Resonances

*Tianxiang Yu,[1#] Mingcheng Panmai,[2#] Shulei Li,[3] Shimei Liu,[1] Yuheng Mao,[1] Lidan Zhou,[4] and Sheng Lan[1]**

1. Guangdong Provincial Key Laboratory of Nanophotonic Functional Materials and Devices, School of Information and Optoelectronic Science and Engineering, South China Normal University, Guangzhou 510006, China

2. School of Electrical and Electronic Engineering, Nanyang Technological University, Singapore 639798, Singapore

3. School of Optoelectronic Engineering, Guangdong Polytechnic Normal University, Guangzhou 510665, China

4. State Key Laboratory of Optoelectronic Materials and Technologies, School of Electronics and Information Technology, Sun Yat-sen University, Guangzhou 51006, China

[#] These authors contributed equally to this work

*Corresponding author: slan@scnu.edu.cn

1. Simulated scattering spectra for a WS_2 nanoparticle placed on a silica (SiO_2) substrate without and with a thin ITO film.

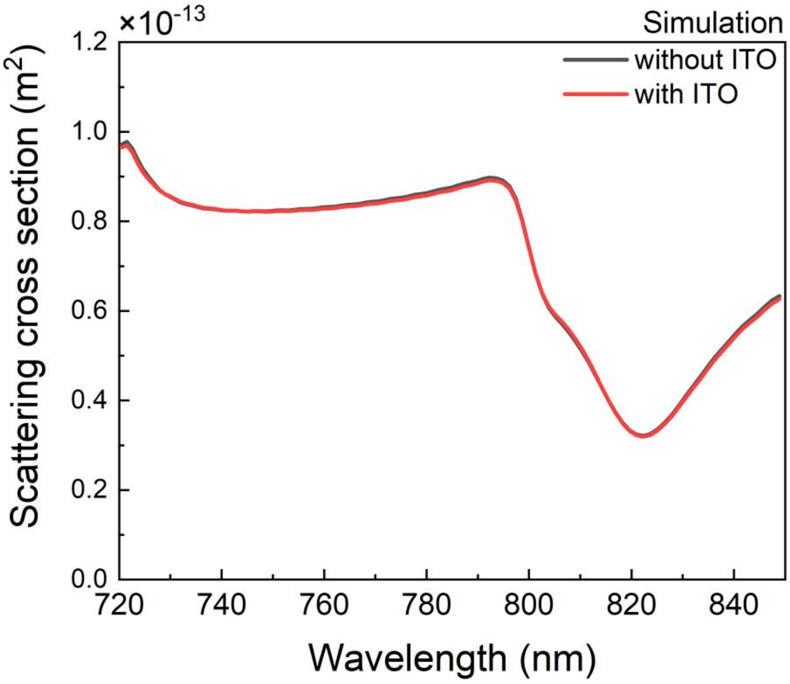

Figure S1. Simulated scattering spectra of a WS_2 nanoparticle placed on a silica (SiO_2) substrate without (black curve) and with (red curve) a thin ITO film of 10 nm.

2. Morphology characterization of WS_2 nanoparticles.

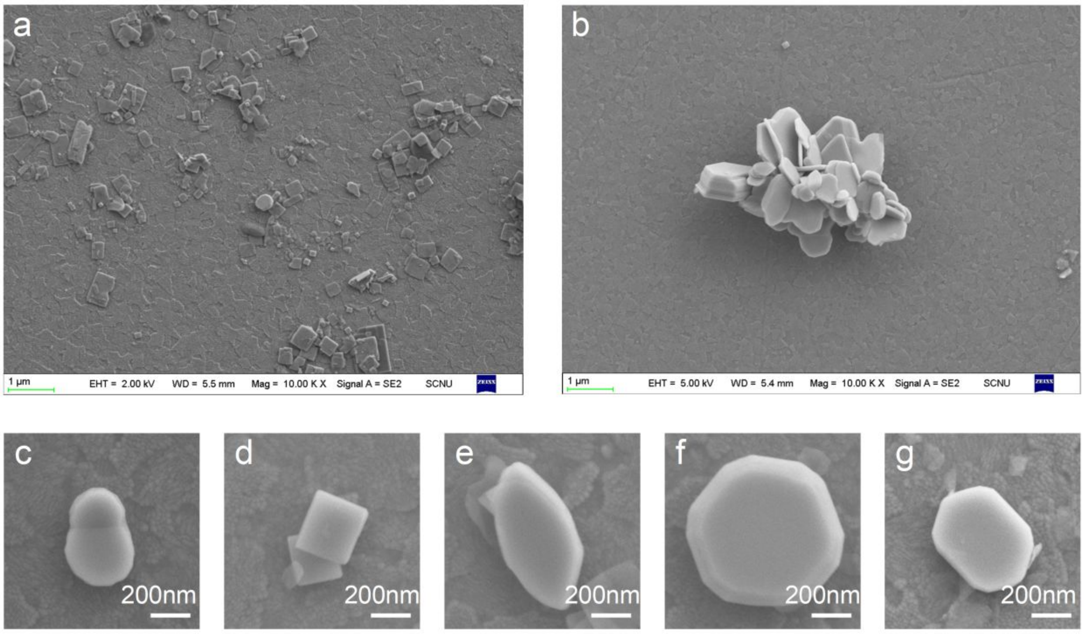

Figure S2. (a-b) SEM images of WS_2 nanoparticles distributed on an ITO/SiO_2 substrate. (c-g) SEM images of single WS_2 nanoparticles with different shapes.

3. SEM images and scattering spectra of more WS_2 nanoparticles

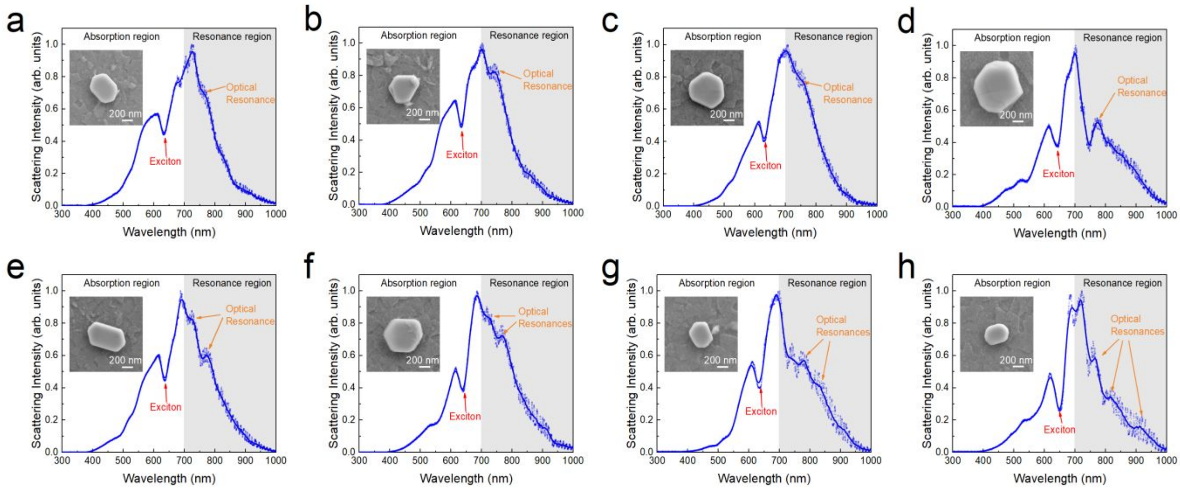

Figure S3. (a-h) Scattering spectrum of more WS_2 nanoparticles. The SEM images of the WS_2 nanoparticles are shown in the insets.

4. Height characterization of WS_2 nanoparticles

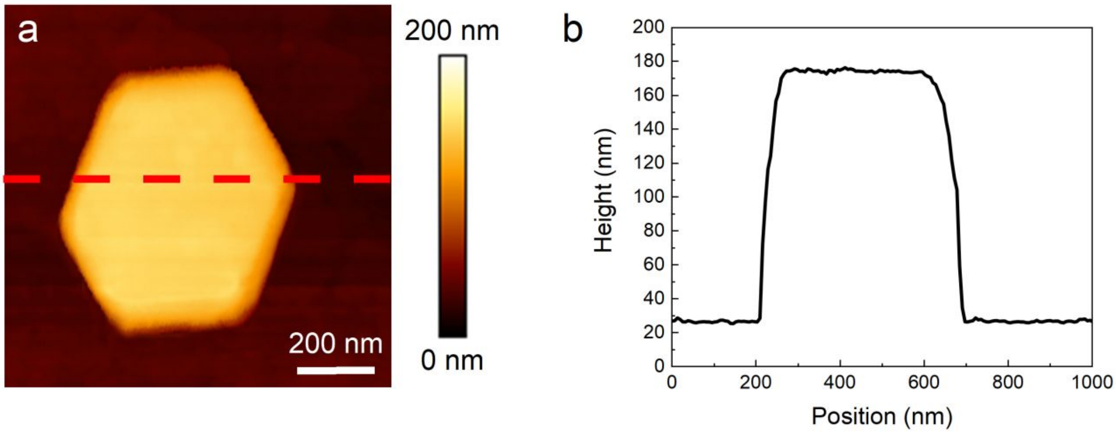

Figure S4. (a) AFM images of the WS_2 nanoparticle shown in Figure 2a. (b) Height profile along the dashed line in (a).

5. Dependence of the SHG intensity of a WS_2 nanoparticle on the pumping power

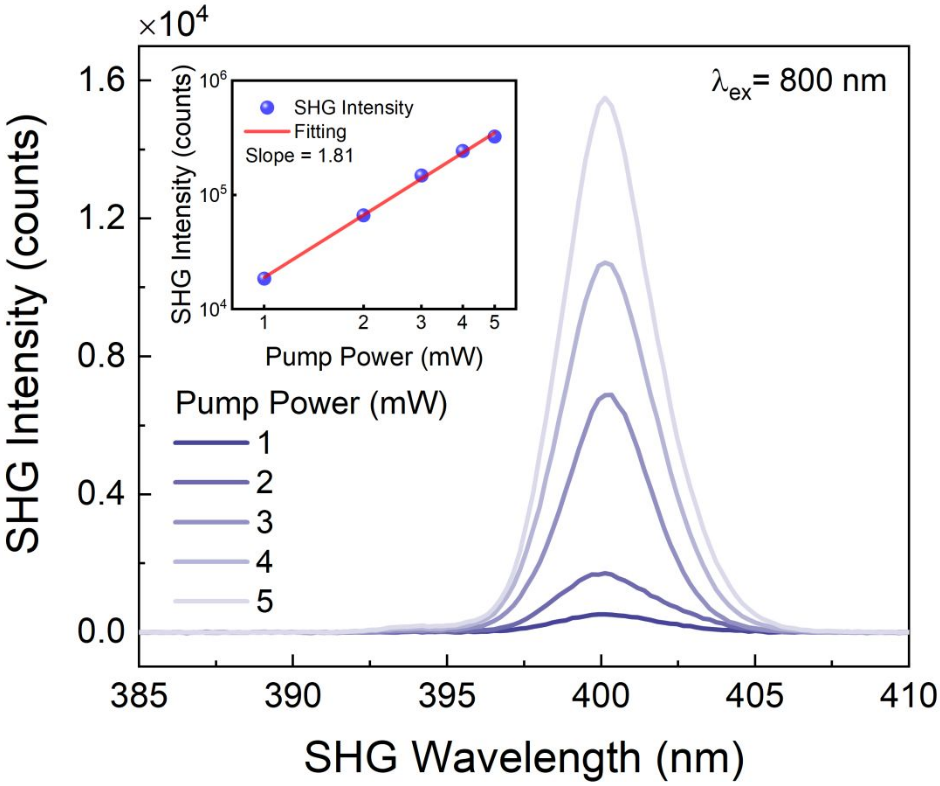

Figure S5. SHG spectra measured for a WS_2 nanoparticle by using femtosecond laser light (λ_{ex} = 800 nm) with different pumping powers. The dependence of the SHG intensity on the pumping power is shown in the inset.

6. Multipolar decomposition of the scattering spectrum of a WS_2 nanoparticle

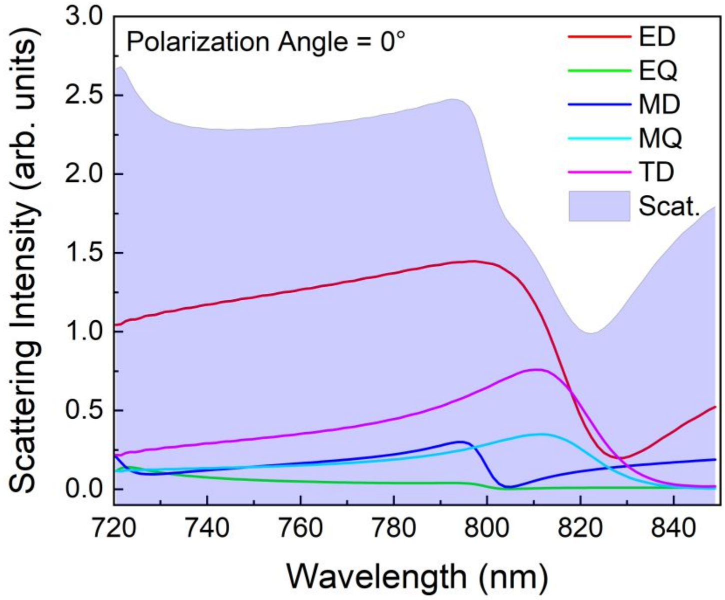

Figure S6. Scattering spectrum simulated for the WS_2 nanoparticle shown in Figure 2 and its decomposition into the Mie resonances. The contribution of TD is included in the decomposition of the scattering spectrum.

7. Dependence of SHG intensity of a WS_2 nanoparticle on the polarization angle of the excitation laser light (λ_{ex} = 775 nm)

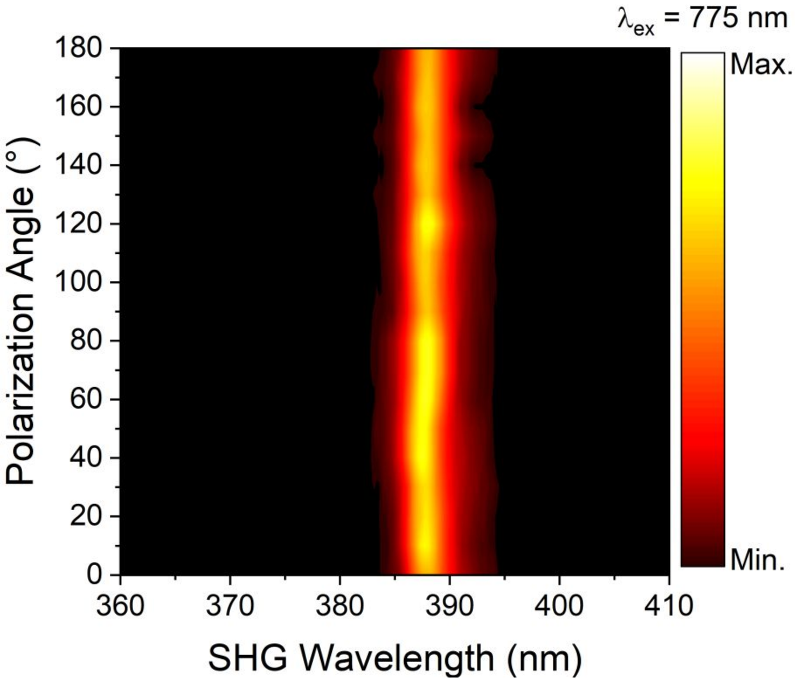

Figure S7: Dependence of the SHG intensity on the polarization angle of the excitation laser light (λ_{ex} = 775 nm) measured for a WS_2 nanoparticle.

8. Polarization-dependent SHG intensity observed in more WS_2 nanoparticles

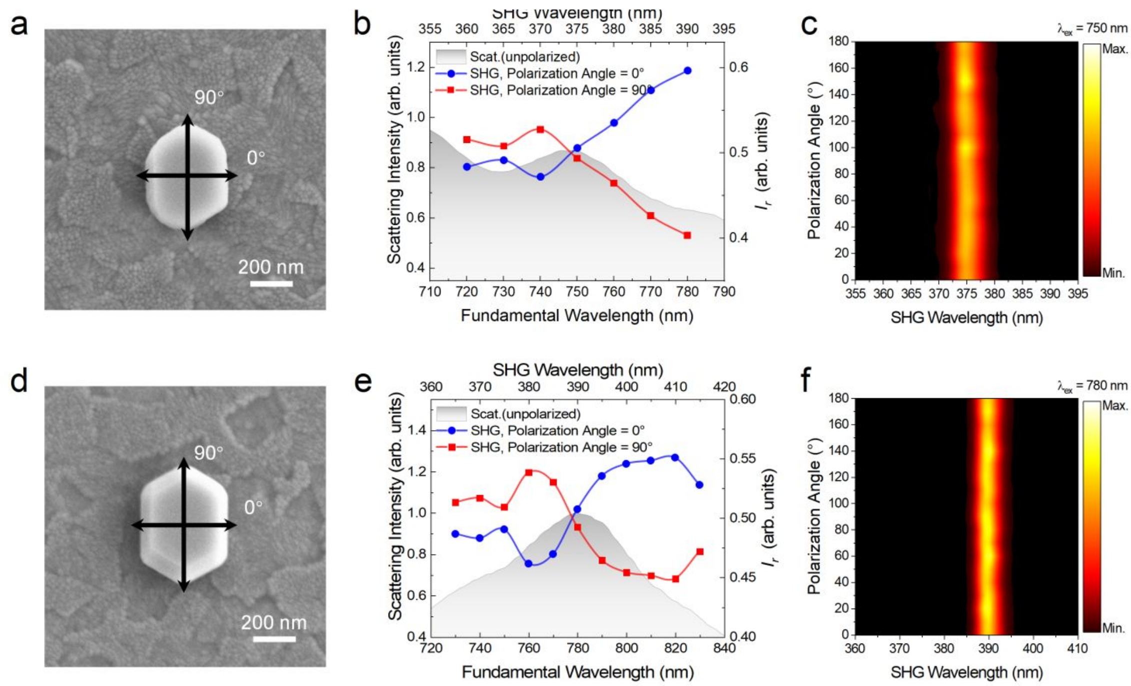

Figure S8. (a), (d) SEM images of another two hexagonal-prism-like WS_2 nanoparticles. (b), (e) Dependence of the relative SHG intensity on the excitation wavelength calculated for the WS_2 nanoparticles at polarization angles of $\theta = 0°$ and $\theta = 90°$. In each case, the scattering spectrum of the WS_2 nanoparticle illuminated with unpolarized white light is provided for reference. (c), (f) Dependence of SHG intensity on the polarization angle of the excitation light observed at the scattering peak. (b) and (c) correspond to (a), (e) and (f) correspond to (d).

9. Evolution of the scattering spectrum with increasing polarization angle and multipole decomposition of the scattering spectrum for a hexagonal-prisms-like WS_2 nanoparticle.

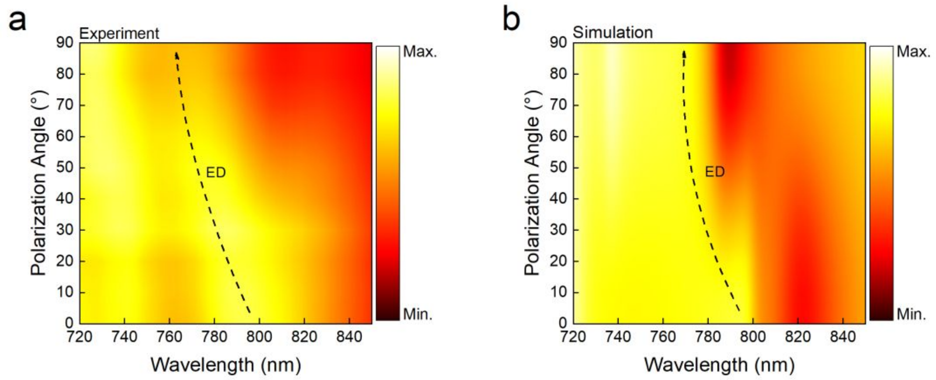

Figure S9. (a-b) Evolution of the scattering spectrum with increasing polarization angle observed for a hexagonal-prisms-like WS_2 nanoparticle. (a) experiment; (b) simulation.

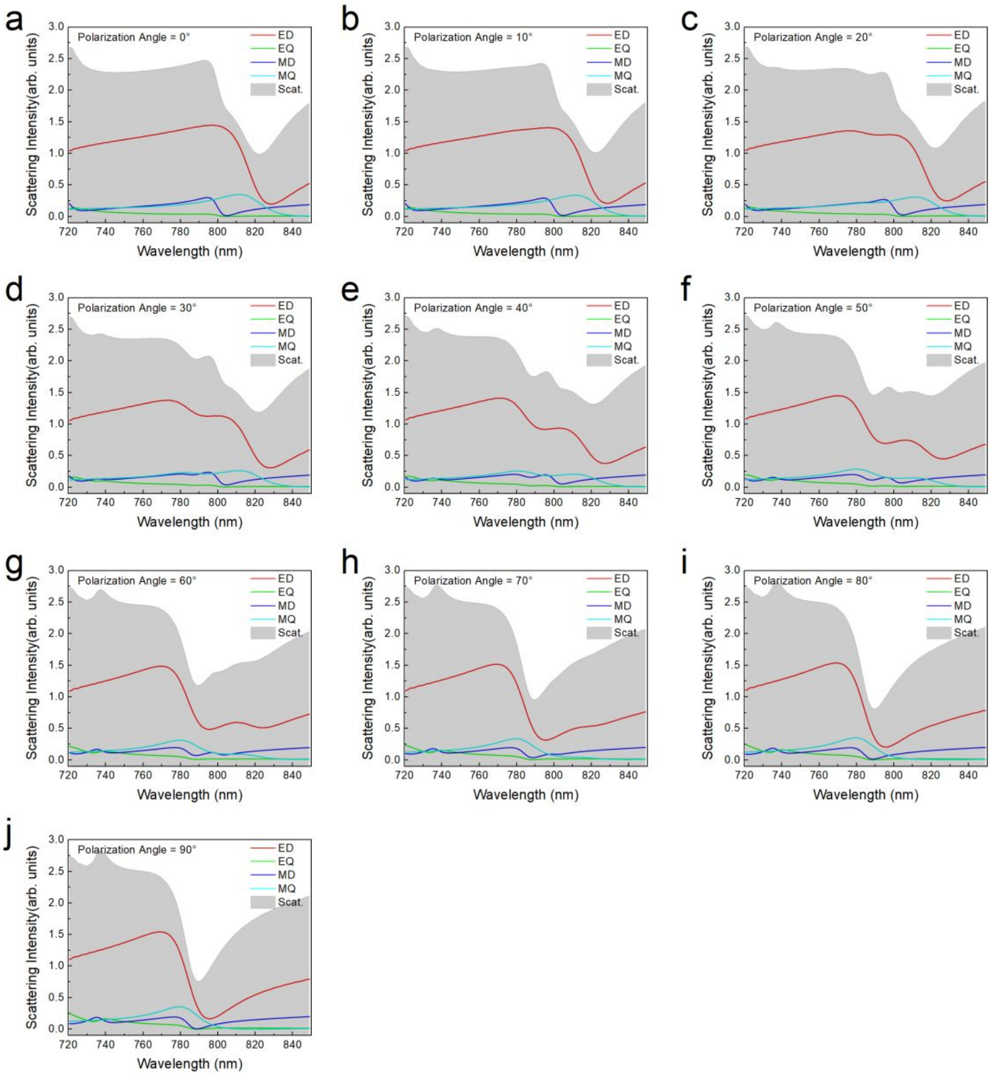

Figure S10. (a-j) Scattering spectra simulated for a hexagonal-prisms-like WS_2 nanoparticle (a = 580 nm, b = 444 nm, c = 312 nm, h = 148 nm) at different polarization angles ranging from $\theta = 0°$ to $\theta = 90°$. In each case, the scattering spectrum is decomposed into the contributions of Mie resonances.

10. Height characterization of WS_2 nanoparticles

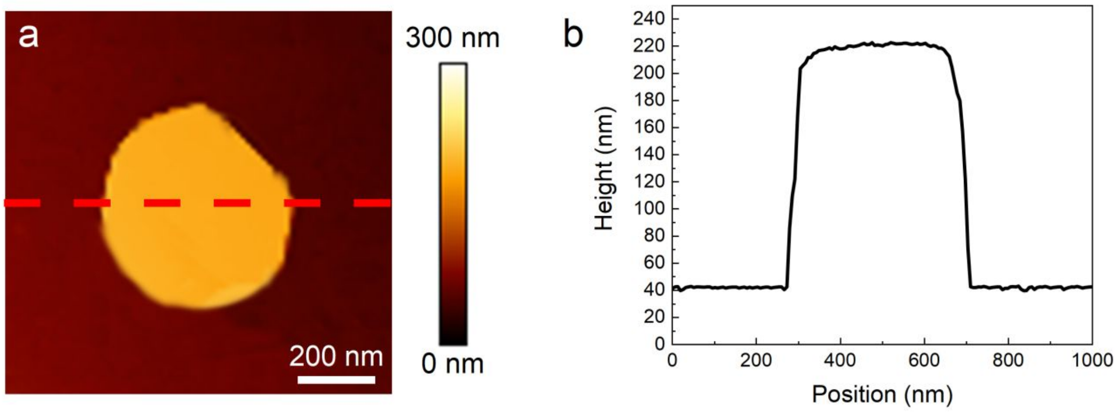

Figure S11. (a) AFM images of the WS_2 nanoparticle shown in Figure 4a. (b) Height profile along the dashed line in (a).

11. Polarization-dependent scattering spectra simulated for a hexagonal-prism WS_2 nanoparticle

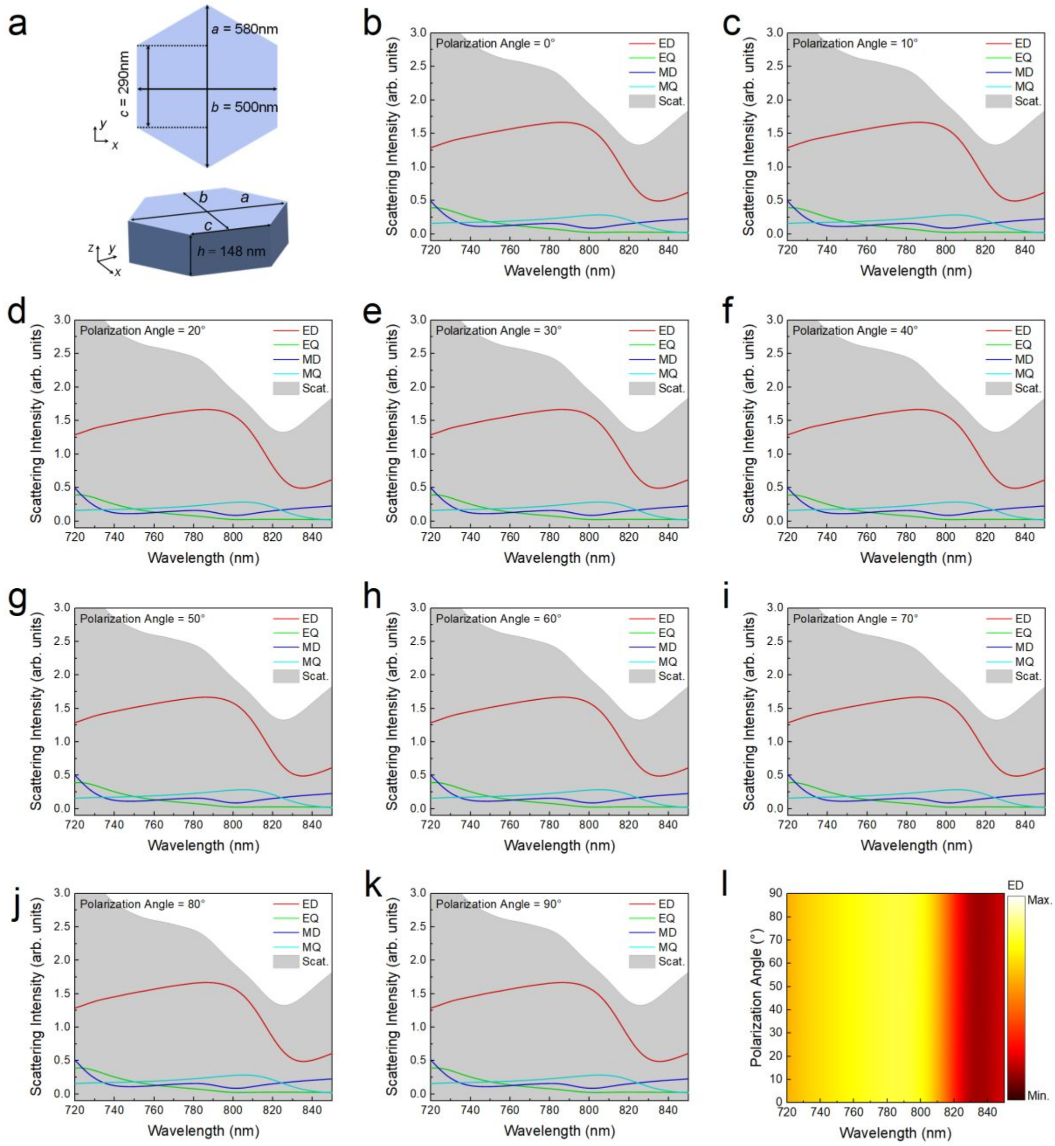

Figure S12. (a) Structure of a hexagonal-prism WS_2 nanoparticle. (b-k) Scattering spectra simulated for the hexagonal-prism WS_2 nanoparticle(a = 580 nm, b = 500 nm, c = 290 nm, h = 148 nm) at polarization angles ranging from $\theta = 0°$ to $\theta = 90°$. In each case, the scattering spectrum is decomposed into the contributions of Mie resonances of different orders. (l) Evolution of the ED resonance with increasing polarization angle simulated for the hexagonal-prism WS_2 nanoparticle.

12. Electric and magnetic field distributions calculated at the optical resonances supported by a hexagonal-prism WS_2 nanoparticle

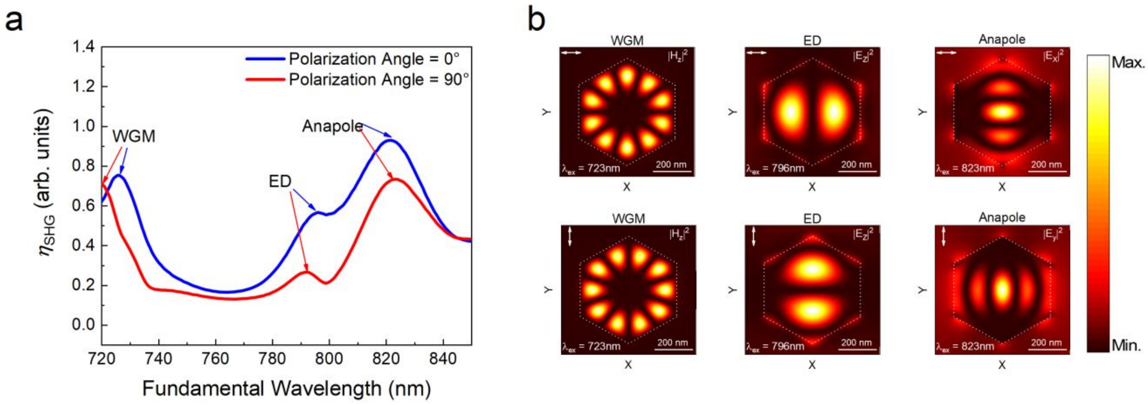

Figure S13. (a) Dependence of the SHG efficiency on the excitation wavelength simulated for the hexagonal-prism WS_2 nanoparticle(a = 580 nm, b = 500 nm, c = 290 nm, h = 148 nm) at polarization angles of θ = 0°and θ = 90°. (b) Electric/magnetic field distributions calculated at different optical resonances. In each case, the polarization of the excitation light is indicated by an arrow.

13. Dependence of the SHG intensity on the polarization angle observed for a WS_2 monolayer

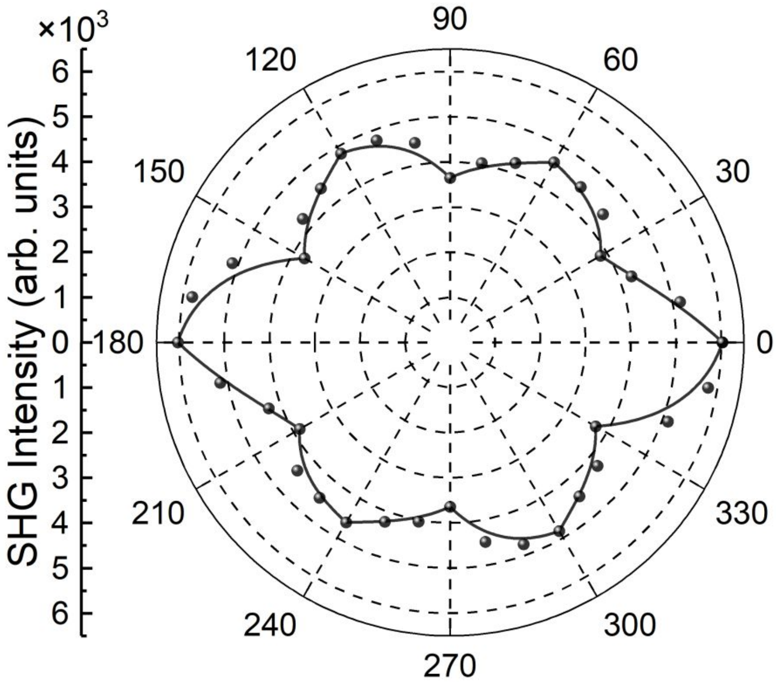

Figure S14. SHG intensities measured for a WS_2 monolayer at different polarization angles.

14. Analysis of the crystal structure of WS_2

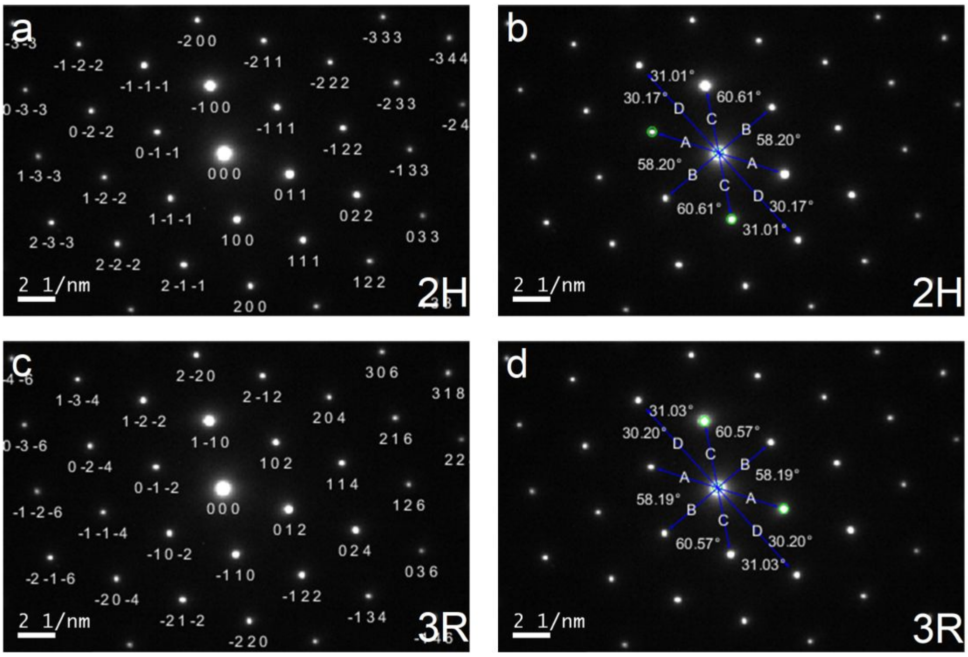

Figure S15: Comparison of the electron diffraction pattern with 2H (a,b) and 3R (c,d).

Table S1: Parameters extracted from the electron diffraction of the WS_2 nanoparticle

polymorph	2H	3R
d spacing	A: 0.277 B: 0.276 C: 0.285 D: 0.163	A: 0.278 B: 0.276 C: 0.285 D: 0.163
Total angular dist.	0.52	1.82
d-spacing STDEV	0.0014	0.0022

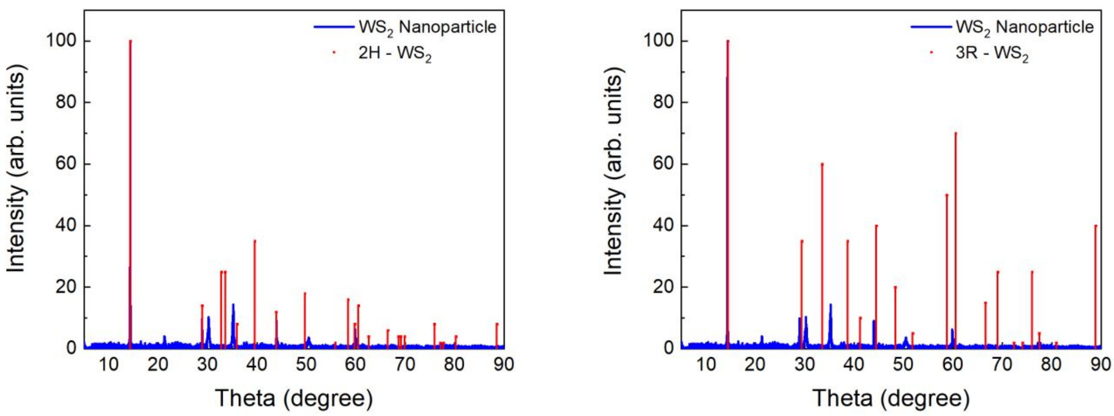

Figure S16. Comparison of the X-ray diffraction spectrum measured for the WS_2 nanoparticle with those of 2H and 3R phases.